Polish Journal of Veterinary Sciences Vol. 23, No. 2 (2020), 301–308

DOI 10.24425/pjvs.2020.133645

Original article

An approximate mathematical model binding the height and position of lumbar vertebrae in the canine spine

I. Wadowska[1], M. Dzierzęcka[1], S. Paśko[2], K. Barszcz[1], B.J. Bartyzel[1]

[1] Faculty of Veterinary Medicine, Department of Morphological Science, Warsaw University of Life Sciences, Nowoursynowska 166, 02-776, Warsaw, Poland
[2] Faculty of Mechatronics, Virtual Reality Techniques Division, The Institute of Micromechanics and Photonics, Warsaw University of Technology, Św. Andrzeja Boboli 8, 02-525, Warsaw, Poland

Abstract

The lumbosacral region of the spine is the most susceptible to pathology in large breed dogs. The most common pathologies of this segment include intervertebral disc disease, distortion of vertebrae, narrowing of the lumbosacral canal and congenital defects of the spine. The aim of this study is to develop a mathematical model describing the height of each lumbosacral vertebra in the dog in relation to the position of the vertebra. For the mathematical analysis we used the results of two measurements for each lumbar vertebra. The first measurement was made from the top of the spinous process to the center of the spinal cord. The second measurement was made from the center of the body of one vertebra to the center of the body of the next one. It is possible to determine an approximate mathematical model that would be uniform for the entire species and would connect the height of the lumbar vertebrae with their location for every breed of the domestic dog. Despite the considerable differences in the constitutional type (small, medium and large breeds), the morphology of the lumbosacral region of the spine exhibits similar proportions. Therefore, it is possible to assess an anomaly of this spinal region objectively. These findings suggest that it is possible to determine an approximate mathematical model that would be uniform for the entire species. The present study was carried out as part of a larger project. This particular work is a pilot study.

Key words: lumbar vertebrae, spine, dogs, mathematical model

Correspondence to: I. Wadowska, e-mail: iza.wadowska@wp.pl

Introduction

Modern radiology currently relies on three diagnostic methods allowing for a precise assessment of bone structures and changes in the intervertebral discs and in the intraspinal structures. These methods include: X-ray, computed tomography (CT), and magnetic resonance (MR) imaging.

The standard lumbosacral diagnostics for dogs has so far been based on X-ray examination. X-ray imaging mainly shows degenerative-productive changes in the skeleton, indirect signs of disc disease, and early stages of disc degeneration. Significant advances in vertebral column visualization and examination were made with the introduction of computed tomography (CT). The major advantages of this method include the possibility of obtaining cross-section images of the body for layers with a thickness of several millimeters, in which the cross-sections of specific organs are shown in accordance with their spatial distribution, as well as the possibility of obtaining a 3D image of the structure under examination on which further analysis can be performed (Paśko et al. 2016, Pankowski et al. 2018). Moreover, due to the higher sensitivity of the radiation sensor, compared to X-ray film, the CT technique offers greater contrast of the organ images (Thrall 2018). Additionally, the use of a contrast medium with CT allows for imaging non-mineralized structures, such as herniated soft tissues of the intervertebral disc. (Niemand et al. 2011).

In recent years, the vertebral column and associated structures are increasingly examined using magnetic resonance imaging (MRI). Unlike CT, MRI is not based on the use of ionizing radiation. The imaging is performed by measuring hydrogen proton resonance signals from the tissue studied. MRI offers excellent contrast resolution for soft tissues and is highly sensitive to any variations, e.g. enabling differentiation between an edema and a hemorrhage. Thus, the method is particularly useful for diagnostics in the central nervous system, nasal cavities and sinuses, joints, and the abdominal cavity (Hecht et al. 2010, Dennis 2011, Kealy et al. 2011). It is also a very good instrument for imaging the alterations associated with intervertebral disc degeneration (Dennis 1998, Tobias et al. 2004, Amort et al. 2012, Freeman et al. 2012).

In human medicine, non-invasive 3D or 4D imaging methods are increasingly used for diagnostics, spinal pathology assessment, follow-up examinations, screening and spine rehabilitation monitoring. Three-dimensional analysis of the spine combines modern optical technology and digital data processing, allowing for automatic, contactless measurement and analysis of the spine. Most importantly, it does not involve the use of harmful radiation, which means the test can be performed more often than conventional X-ray examinations (Drerup and Hierholzer 1987, 1996, Hackenberg et al. 2003, Sutkowski et al. 2017). It allows us to see various clinical parameters using static body analysis. However, to fully use this method we need mathematical models comparing the parameters of individual parts in the spine (Drerup and Hierholzer 1987, 1996). There are several publications in human medicine about the use of mathematical models (Aspden 1988, Stambough et al. 1995, Humbert et al. 2007, Voinea et al. 2017). For example, we can use such models in medical rehabilitation sessions and to help patients to avoid incorrect postures (Voinea et al. 2017). These techniques also appear more and more often in animal medicine.

Each of these methods focuses on different structures under diagnosis, and none is perfect, hence the importance of investigating new diagnostic imaging methods. The greatest shortcomings of imaging methods include the need for sedation and radiation. This is particularly important in chronically ill individuals that undergo follow-up examinations frequently.

It has been demonstrated that in large dog breeds, the lumbosacral region of the spine is the most susceptible to pathology (Ziegler 1989, Morgan et al. 1993, Morgan 1999, Breit et al. 2003, Damur-Djuric et al. 2006, Flückiger et al. 2006, Amort et al. 2012, Lappalainen et al. 2012). The most common is intervertebral disc degeneration, which is caused on a cellular level by alterations in the cell cycle and transformation. The number of notochordal cells in the disc decreases as the cells mature more quickly, cell composition changes, cellular matrix homeostasis is disturbed, and the matrix enzyme function is impaired. These processes contribute to cellular matrix degeneration (Glinkowski and Ciszek 2004, Bergknut et al. 2013). The German Shepherd is one of the breeds most susceptible to the pathologies described above (Jones et al. 2000, Seiler et al. 2002, Amort et al. 2012, Gomes et al. 2016).

In one study, 110 clinically healthy German Shepherds and 47 dogs of other breeds of a similar size and habitus were examined using MRI. Their lumbosacral spine was examined using a four-grade system for disc degeneration classification (Seiler et al. 2002, Amort et al. 2012). Among the German Shepherds, 50% of the animals were found to have grade 3 degeneration, and 26% had grade 4 degeneration. In a randomly selected population of clinically healthy dogs of other breeds, only grade 2 degeneration was found, which affected 62% of the animals studied (Amort et al. 2012). Intervertebral disc degeneration can lead to spinal stenosis which, in the lumbosacral region, may

cause compression of the spinal nerve roots of cauda equina. Compression of these nerves (sciatic, pudendal, pelvic, and caudal) may lead to pelvic limb paresis, tail paralysis, and urinary dysfunction. The symptoms, termed the cauda equina syndrome (CES), may have various causes, including congenital defects or acquired pathologies (Palmer et al. 1991, Lang et al. 1992). CES is also associated with a hereditary or congenital anomaly called lumbosacral transitional vertebra (LTV). Transitional vertebrae are improperly shaped vertebrae that resemble those of an adjacent regions. These changes can affect the whole vertebra or part of it. The term LTV is a vertebra located between a normally developed the last lumbar vertebra and the first sacral vertebra. If the first sacral vertebra (S1) is deformed and has anatomical features of the lumbar vertebra, we call it lumbarization of the first sacral vertebra. If the change refers to the seventh lumbar vertebra (L7) we call it sacralisation of the lumbar vertebra (Flückiger et al. 2006, Niemand 2011, Lappalainen et al. 2012). The presence of LTV in dogs predisposes them to early lumbosacral junction degeneration, which in turn leads to CES (Niemand 2011). Again, German Shepherds are predisposed to LTV, which is up to 8 times more common than in other breeds (Morgan et al. 1993, Morgan 1999, 2006, Flückiger et al. 2006). LTV is also relatively common in Labrador Retrievers (Breit et al. 2003), Chow-Chows (Ziegler 1989), Dobermanns (Ziegler 1989), and Greater Swiss Mountain Dogs (Damur-Djuric et al. 2006).

Literature data unambiguously confirm a breed-specific predisposition to lumbosacral pathology in the species. Therefore, detailed understanding of the morphology and morphometry of each element of this spinal region is extremely important. However, no detailed studies including a description of the structure of lumbosacral vertebrae, performed using sufficiently diverse material, are available so far. It is these considerations, combined with potential cognitive value, that motivated the present study. Detailed measurements of each vertebra of the lumbosacral region, which is the most prone to injury, are of clinical importance, as they allow for an objective assessment of the structure of the canine spine. Hence this analysis, aimed at developing a mathematical model describing the height of each lumbosacral vertebra in the domestic dog in relation to the position of the vertebra. A mathematical model representing the morphology of vertebrae in a given spinal region is a very useful and objective diagnostic instrument. So far, such a model has only been developed for humans, which means the present study is a pioneering one in veterinary medicine. The development of a mathematical model representing normal values for each vertebra may also accelerate the detection of anomalies and predisposition to spinal pathology.

Materials and Methods

The present study initiates a project that will be implemented in the future. The aim of this pilot study is to verify whether the method proposed by the authors is correct.

Animal models

Research material was collected from dogs of various breeds (n=105), including 58 males and 47 females. Images were obtained in the years 2014 - 2017. The dogs were aged between 1 and 17 years, and weighed between 3 and 72 kg. A number of individuals were selected based on similar research done in human medicine. All dogs selected for the study were random individuals. In order for the measurements to be performed correctly, only dogs with serious defects were rejected e.g. French Bulldogs with hemivertebrae.

Pet owners and owners of veterinary clinics for animals were informed about the tests. The personal data of the owners were not included in the survey. Data collected from animals include: name, race, age, weight and gender.

X-ray images

Dogs included in the study had radiographic examination of the lumbosacral spine for different reasons (check-up, lumbar pain or suspected disease). However, no dog was examined only to be included in the study. X-ray images were selected according to specific criteria. The first criterion was the method of taking the image (description below). The second criterion was the dog's breed. The most common breeds were selected.

The digital X-ray images for measurements were produced at small animal clinics in Warsaw, using the EXAMION® Maxivet 300 HF system. Depending on the individual dog's size, the voltage ranged between 76 and 54 kV, and the current ranged between 16 and 20 mAs. These values were used for a film-focus distance of 100 cm. All X-ray images were taken by radiologists and one of the authors of the present paper. During the X-ray examination, the animals were in the left lateral position. The limbs were placed caudally and secured with a sandbag. The head was kept in natural position with support for the neck with foam or a sandbag. The collimation included T12 and S1. The central ray was directed at L4. Before the examination, dogs

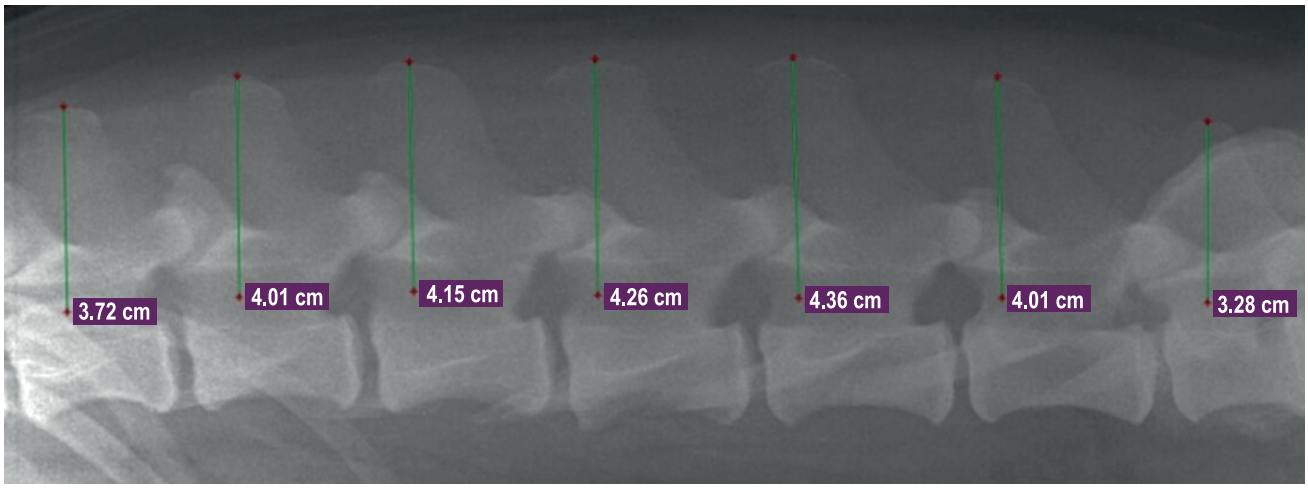

Fig. 1. First measurement line - from the tip of the spinous process to the center of the spinal cord. Dog, Labrador Retriever, 7 years old, female, 33 kg.

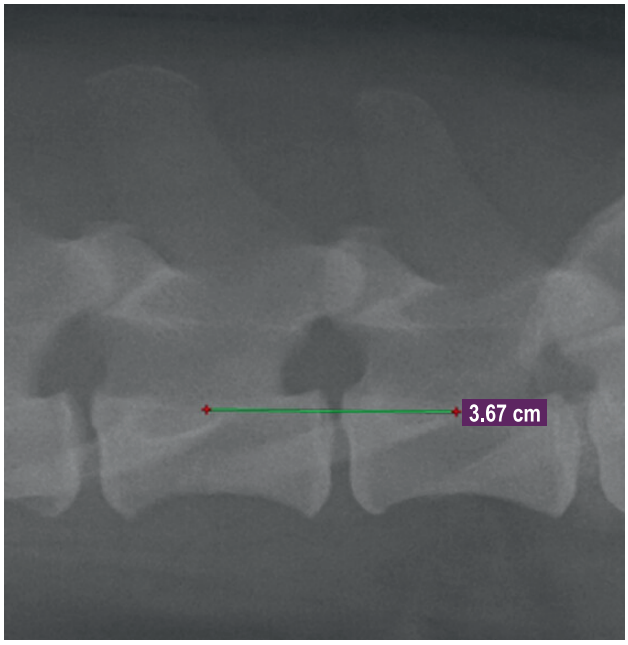

Fig. 2. Second measurement line - from the center of the body of one vertebra to the center of the body of the next. Measurement made between vertebrae L6 and L7. Dog, Labrador Retriever, 7 years old, female, 33 kg.

were tranquilized using a mixture of medetomidine (Dexdomitor, 0.01-0.02 mg/kg bw), butorphanol (Morphasol, 0.1-0.5 mg/kg bw) and ketamine (Vetaketam, 2-5mg/kg bw), administered intramuscularly.

Two measurements were made in the X-ray images for each lumbar vertebra. The first measurement was made from the top of the spinous process to the center of the spinal cord (Fig. 1). The second measurement was made from the center of the body of one vertebra to the center of the body of the next one (Fig. 2). Measurements were made using the RadiAnt DICOM Viewer software.

Mathematical analysis

The results of the two measurements of each lumbar vertebra in each animal were used for mathematical analysis. Data from the second measurement, i.e. the distance between the centers of the bodies of each two adjacent vertebrae, were used to calculate the distance between the first vertebra and each subsequent one. Assuming that n is the index of a vertebra, N is the number of vertebrae or the index of the last vertebra, and $d_{n,n-1}$ is the distance between a vertebra and the previous one, the above-mentioned distance from the first vertebra, $d_{n,1}$, is described by the following expression.

Data from the first measurement, i.e. the height of the vertebrae, were noted as h_n. These data were used

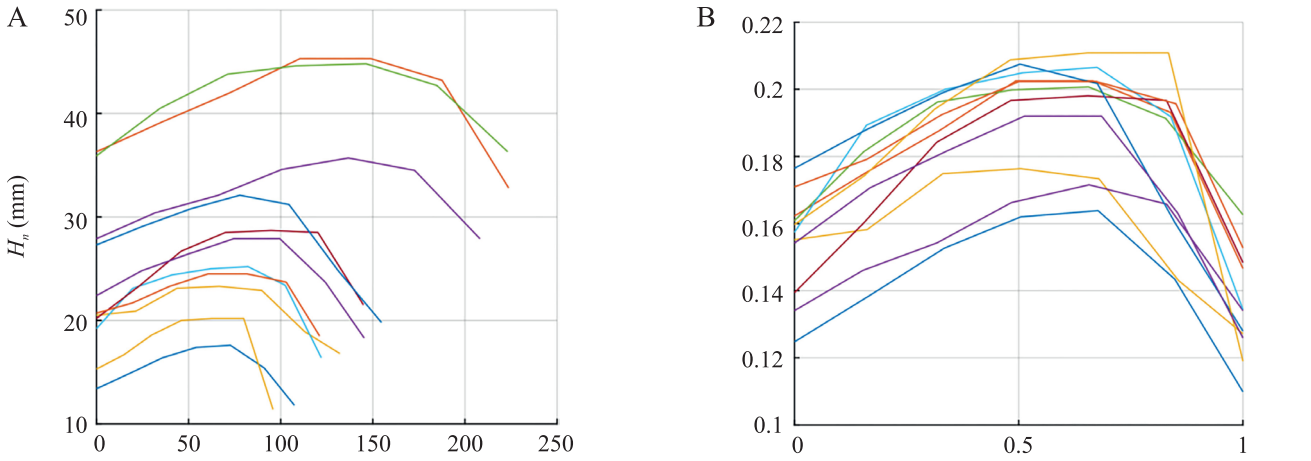

Fig. 3. Distance between the tip of the spinous process and the center of the spinal cord, as a function of position relative to the center of the first vertebra analyzed; A) without normalization for 10 cases, B) normalized.

Table 1. Coefficients of the second-, third-, and fourth-degree polynomials for curve fitting to parameters describing the canine lumbar vertebrae.

degree polynomials	a_4	a_3	a_2	a_1	a_0
4	0.1264	-0.4329	0.2329	0.0537	0.1599
3	-	-0.1801	0.0768	0.0834	0.1594
2	-	-	-0.1930	0.1830	0.1544

directly in the analysis. The distribution of vertebral height h_n as a function of distance $d_{n,1}$ is shown in the chart (Fig. 3A). For the sake of clarity, only data for 10 randomly selected measurements are visualized.

For each animal, the measured distances were normalized by dividing both the vertebral height h_n and the distance from the first vertebra $d_{n,1}$ by $d_{N,1}$. Normalized distances h_n and $d_{n,1}$ are noted as $H_n = \frac{h_n}{d_{N,1}}$ and $D_n = \frac{d_n}{d_{N,1}}$.

The results of these calculations are shown in Fig. 3B. Subsequently, second-, third-, and fourth-degree polynomials were fitted to the data expressed as $H_n(D_n)$, using the *fit* function of the Matlab package. The notation used for the polynomials is shown using the example of a fourth-degree polynomial.

$$y = a_4x^4 + a_3x^3 + a_2x^2 + a_1x + a_0$$

The "QR factorization and solve" algorithm was used for the calculations. Analyses were performed to select the polynomial with the lowest possible order and the least possible error. Because H_n for each animal has a different value at $D_{1,1}$ (0 on the X axis), the a_0 parameter of the polynomial was determined based on this value, using nonlinear regression. This ensures a better fit of the model to the case being analyzed. Relative distances were converted into absolute distances in each case by multiplying the polynomial by a constant, $d_{n,1}$.

Results

The results of second-, third-, and fourth-degree polynomial fitting to data expressed as $H_n(D_n)$ are shown in Table 1.

The chart in Fig. 4 shows the third degree polynomial curve against the data expressed as $H_n(D_n)$ for all the animals studied.

As the parameters may vary significantly, even by twice as much, between the individuals studied, a relative, percentage-based analysis was performed. For each polynomial at $d_{n,1}$, the mean percentage deviation of the model curve from the actual value was calculated for the entire set of cases. The calculation results are shown in Table 2.

The lowest percentage deviation between the model and the actual value for subsequent vertebrae was found with a third-degree polynomial. Therefore, the canine lumbar spine model is described by the following expression:

$$h_n = -0.1801d_{n,1}x^3 + 0.0768d_{n,1}{}^2 + 0.0834d_{n,1} + a_0,$$

where a_0 is calculated by fitting the model to the data using nonlinear regression.

Discussion

The present study shows that for six out of the seven lumbar vertebrae, 90% of measurements fall within a 10% error margin. For the last vertebra, the error was

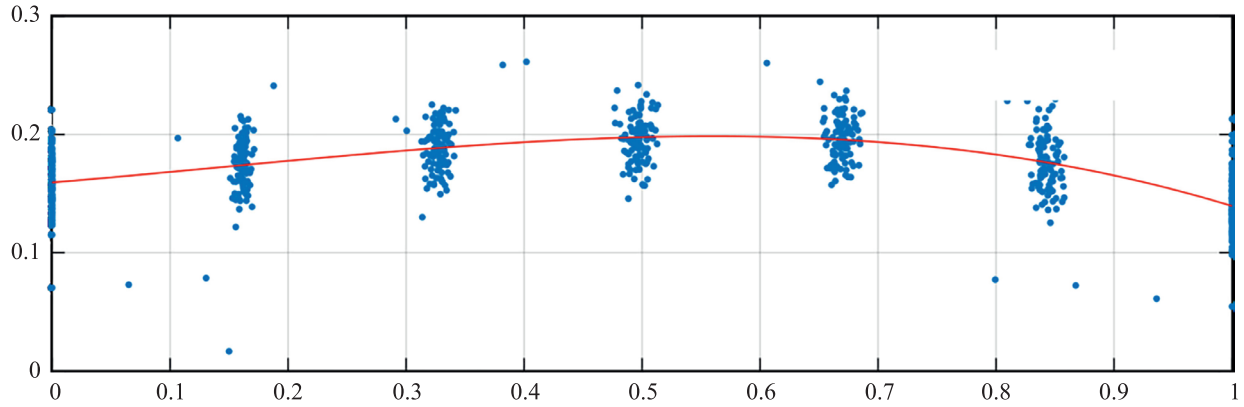

Fig. 4. Third-degree polynomial fitted to parameters describing the canie lumbar vertebrae.
The chart in Fig. 4 shows the third-degree polynomial curve against the data expressed as $H_n(D_n)$ for all the animals studied.

Table 2. Mean percentage deviation of the model from the actual values for subsequent vertebrae.

degree polynomials	vertebra 1 [%]	vertebra 2 [%]	vertebra 3 [%]	vertebra 4 [%]	vertebra 5 [%]	vertebra 6 [%]	vertebra 7 [%]
4	3.7	3.1	2.5	3.2	2.2	4.8	6.8
3	3.7	3.0	2.5	3.1	2.2	4.7	6.8
2	4.5	3.9	3.6	3.0	3.3	5.3	6.6

larger, up to 14%. This may indicate that this vertebra accounts for most diversity in the parameters of the dog lumbar spine.

Distribution anomalies were found in three dogs with a body weight below 14 kg. Minor anomalies were also found in another dog of the miniature type. This may suggest that spinal deformations appeared in these dogs either prenatally or during later development. Deviations from the norm were mainly found in dogs of smaller breeds, which may suggest that lumbar spine deformities occur more often in these breeds than in others, though such a hypothesis requires verification in a larger population of miniature dogs. On the other hand, such a small percentage of animals whose body build diverges from the norm (3.8 %) means that it is possible to formulate a mathematical model for canine lumbar spine, as has been the case for humans (Drerup and Hierholzer 1987, 1996). Many studies report a significant correlation between the structure of vertebrae and predisposition to spinal disease.

Recent findings indicate that in dogs with a lumbosacral transitional vertebra (LTV), the L7 is longer than L6, in contrast to healthy dogs. Additionally, a decrease of the L6/L7 ratio by 0.1 increases the likelihood of L8 occurrence fourteen times (Dennis 2011).

Notably, dogs with LTV are also eight times more likely to develop the cauda equina syndrome, which also occurs approximately 1.5 years earlier in these dogs than in dogs without LTV (Dennis 2011).

Previous measurements of the lumbar spine mainly focused on establishing normal reference ranges for the spinal cord and spinal canal diameter, and were made using MRI in healthy dogs (Hecht et al. 2014).

No literature data are available regarding other parameters of vertebral structure.

Use of imaging techniques in studies requires not only the technical skills for obtaining the images, but also the ability to interpret correctly the images obtained using the various techniques. Accurate images suitable for scientific analysis can only be obtained if the test parameters are set correctly, in accordance with reference values for specific breeds. In the present study, measurements were performed in order to establish the normal reference ranges for the size of each lumbar vertebra in dogs. The findings will be a valuable contribution to current knowledge on canine spine anatomy, physiology and biomechanics. In the future, they will allow precise analysis of changes in the vertebral structures resulting from pathological processes in the given region of the spine. The mathematical model presented may be used for quick spine assessment, both clinically and using X-ray images, which in turn may contribute to early diagnosis of even slight alterations in the spine, resulting in early treatment.

Conclusions

Despite the considerable breed diversity of the domestic dog (*Canis lupus f. familiaris s. Canis lupus f. domestica*), it is possible to determine an approximate mathematical model that would be uniform for the

entire species and would connect the height of the lumbar vertebrae with their location for every breed.

It was also shown that despite the considerable differences in the constitutional type (small, medium and large breeds), the morphology of the lumbosacral region of the spine exhibits similar proportions. Therefore, it is possible to assess the anomaly of this spine region objectively. However before the use of the model in predicting or diagnosing of the canine lumbosacral anomalies, further studies have to be carried out.

References

Amort KH, Ondreka N, Rudorf H, Stock KF, Distl O, Tellhelm B, Kramer M, Wigger A (**2012**) MR - imaging of lumbosacral intervertebral disc degeneration in clinically sound german shepherd dogs compared to other breeds. Vet Radiol Ultrasound 53: 289-295.

Aspden RM (**1988**) A new mathematical model of the spine and its relationship to spinal loading in the workplace. Appl Ergon 19: 319-323.

Bergknut N, Meij BP, Hagman R, de Nies KS, Rutges JP, Smolders LA, Creemers LB, Lagerstedt AS, Hazewinkel HA, Grinwis GC (**2013**) Intervertebral disc disease in dogs - part 1: a new histological grading scheme for classification of intervertebral disc degeneration in dogs. Vet J 195: 156-163.

Breit S, Knaus I, Kunzel W (**2003**) Differentiation between lumbosacral transitional vertebrae, pseudolumbarisation, and lumbosacral osteophyte formation in ventrodorsal radiographs of the canine pelvis. Vet J 165: 36-42.

Damur-Djuric N, Steffen F, Hassig M, Morgan JP, Flückiger MA (**2006**) Lumbosacral transitional vertebrae in dogs: Classification, prevalence, and association with sacroiliac morphology. Vet Radiol Ultrasound 47: 32-38.

Dennis R (**1998**) Magnetic resonance imaging and its applications in small animals. In Practice 20: 117-124.

Dennis R (**2011**) Optimal magnetic resonance imaging of the spine. Vet. Radiol. Ultrasound 52: 72-80.

Drerup B, Hierholzer E (**1987**) Automatic localization of anatomical landmarks on the back surface and construction of a body-fixed coordinate system. J Biomech 20: 961-970.

Drerup B, Hierholzer E (**1996**) Assessment of scoliotic deformity from back shape asymmetry using an improved mathematical model. Clin Biomech 11: 376-383.

Freeman AC, Platt SR, Kent M, Howerth E, Holmes SP (**2012**) Magnetic resonance imaging enhancement of intervertebral disc disease in 30 dogs following chemical fat saturation. J Small Anim Pract 53: 120-125.

Flückiger MA, Damur-Djuric N, Hassig M, Morgan JP, Steffen F (**2006**) A lumbosacral transitional vertebra in the dog predisposes to cauda equina syndrome. Vet Radiol Ultrasound 47: 39-44.

Glinkowski W, Ciszek B (**2004**) Morphology and properties of intervertebral discs-selected issues (part I). Ortop Traumatol Rehab 6: 141-148.

Gomes SA, Volk HA, Packer RM, Kenny PJ, Beltran E, De Decker S (**2016**) Clinical and magnetic resonance imaging characteristics of thoracolumbar intervertebral disk extrusions and intervertebral disk protrusions in large breed dogs. Vet. Radiol. Ultrasound 57: 417-426.

Hackenberg L, Hierholzer E, Pötzl W, Götze C, Liljenqvist U (**2003**) Rasterstereographic back shape analysis in idiopathic scoliosis after posterior correction and fusion. Clin Biomech (Bristol, Avon) 18: 883-889.

Hathcock JT, Pechman RD, Dillon AR, Knecht CD, Braund KG (**1988**) Comparison of three radiographic contrast procedures in the evaluation of the canine lumbosacral spinal canal. Vet Radiol Ultrasound 29: 4-15.

Hecht S, Adams WH (**2010**) MRI of brain disease in veterinary patients part 1: basic principles and congenital brain disorders. Vet Clin North Am Small Anim Pract 40: 21-38.

Hecht S, Huerta MM and Reed RB (**2014**) Magnetic resonance imaging (MRI) spinal cord and canal measurements in normal dogs. Anat Histol Embryol 43: 36-41.

Humbert L, De Guise JA, Aubert B, Godbout B, Parent S, Mitton D, Skalli W (**2007**) 3D Reconstruction of the Spine from Biplanar X-rays. J Biomech 40: 160.

Jones JC, Inzana KD (**2000**) Subclinical CT abnormalities in the lumbosacral spine of older large-breed dogs. Vet Radiol Ultrasound 41: 19-26.

Kealy JK, McAllister H, Graham JP (**2011**) Diagnostic Radiology and Ultrasonography of the Dog and Cat, 5th Edition. Missouri, Elsevier 9-10.

Lang J, Hani H, Schawalder P (**1992**) A sacral lesion resembling osteochondrosis in the German Shepherd dog. Vet Radiol Ultrasound 33: 69-76.

Lappalainen AK, Salomaa R, Junnila J, Snellman M, Laitinen-Vapaavuori O (**2012**) Alternative classification and screening protocol for transitional lumbosacral vertebra in German shepherd dogs. Acta Vet Scand 54: 27.

Morgan JP, Bahr A, Franti CE, Bailey CS (**1993**) Lumbosacral transitional vertebrae as a predisposing cause of cauda equina syndrome in German shepherd dogs: 161 cases (1987-1990). J Am Vet Med Assoc 202: 1877-1882.

Morgan JP (**1999**) Transitional lumbosacral vertebral anomaly in the dog: a radiographic study. J Small Anim Pract 40: 167-172.

Niemand HG, Suter P, Kohn B, Schwarz G (**2011**) Clinical practice: dogs. Enke, Stuttgart, pp 961-976.

Palmer RH, Chambers J (**1991**) Canine lumbosacral disease. Part I. Anatomy, pathophysiology and clinical presentation. Compend Contin Educ Pract Vet 13: 61-68.

Palmer RH, Chambers J (**1991**) Canine lumbosacral disease. Part II. Definitive diagnosis, treatment and prognosis. Compend Contin Educ Pract Vet. 13: 213-222.

Pankowski F, Paśko S, Max A, Szal B, Dzierzęcka M, Gruszczyńska J, Szaro P, Gołębiowski M, Bartyzel B (**2018**) Computed tomographic evaluation of cleft palate in one-day-old puppies. BMC Vet Res 14: 316.

Paśko S, Bartyzel B, Dzierzęcka M, Murawska D, Szlufik K, Bakoń L, Gruszczyńska J, Grzegrzółka B, Nowicki M (**2016**) Diagnostic Application of Multirow Computed Tomography of the Hip Joint of Japanese Quails (*Coturnix Japonica*). Braz J Poultry Sci 18: 501-504

Pooya HA, Seguin B, Tucker RL, Gavin PR, Tobias KM (**2004**) Magnetic resonance imaging in small animal medicine: clinical applications. Compend Contin Educ Vet 26: 292-301.

Seiler GS, Hani H, Busato AR, Lang J (**2002**) Facet joint

geometry and intervertebral disk degeneration in the L5-SI region of the vertebral column in German shepherd dogs. Am J Vet Res 63: 86-90.

Selcer BA, Chambers JN, Schwensen K, Mahaffey MB (**1988**) Epidurography as a diagnostic aid in canine lumbosacral compressive disease: 47 cases (1981-1986). Vet Comp Orthop Traum 2: 97-103.

Shobeiri E, Khalatbari MR, Taheri MS, Tofighirad N, Moharamzad Y (**2009**) Magnetic resonance imaging characteristics of patients with low back pain and those with sciatica. Singapore Med J 50: 87-93.

Stambough J, Genaidy A, Guo L (**1995**) A mathematical lifting model of the lumbar spine. J Spinal Disord 8: 264-277.

Sutkowski M, Paśko S, Żuk B (**2017**) A study of interdependence of geometry of the nuchal neck triangle and cervical spine line in the habitual and straightened postures. J Anat Soc India 66: 31-36.

Thrall DE (**2018**) Textbook of Veterinary Diagnostic Radiology. 7th ed., Elsevier, Saunders, pp 23-39, 249-306.

Voinea GD, Butnariu S, Mogan G (**2017**) Measurement and Geometric Modelling of Human Spine Posture for Medical Rehabilitation Purposes Using a Wearable Monitoring System Based on Inertial Sensors. Sensors 17: 3.